Ultrafast Intersystem Crossing in 1-Nitronaphthalene. An Experimental and Computational Study

Jimena S. Zugazagoitia, César Xavier Almora-Díaz, and Jorge Peon*

Universidad Nacional Autónoma de México, Instituto de Química, Ciudad Universitaria, 04510, México, D.F., México

Received: June 20, 2007; In Final Form: October 16, 2007

Previous studies have established that the major pathway for the first singlet excited state of 1-nitronaphthalene is intersystem crossing to the triplet manifold. In this contribution we present determinations of the decay of the S_1 state of this compound in several solvents to establish the time scale of the multiplicity change as a function of the polarity and hydrogen-bonding ability of the solvent environment. The measurements were made with the femtosecond frequency up-conversion technique to follow the weak spontaneous molecular emission which precedes triplet formation. Our results show that in all environments the S_1 lifetime is 100 fs or less, making 1-nitronaphthalene the organic compound with the fastest multiplicity change ever measured. We also show that the bathochromic shifts observed for the first absorption band imply changes in the relative energies of the singlet and triplet manifolds, which in turn manifest in a 2-fold increase of the fluorescence lifetime in cyclohexane compared with the polar solvents. Additionally, we performed excited-state calculations at the TD−DFT/ PBE0/6-311++G(d,p) level of theory with the PCM model for solvation. The TD−DFT theory identifies the presence of upper triplet states which can act as receiver states in this highly efficient photophysical pathway. Together, the experimental and theoretical results show that the dynamics of the S_1 state in 1-nitronaphthalene represent an extreme manifestation of El-Sayed's rules due to a partial ($n-\pi^*$) character in the receiver triplets which are nearly isoenergetic with S_1, determining a change in the molecular spin state within 100 fs.

Introduction

When a NO_2 group is directly bonded to a polycyclic aromatic system, the photophysics and the photochemistry of the molecule are drastically changed by this substituent. The primary pathways after excitation to the first singlet excited state in these compounds include, as the main channel, rapid intersystem crossing to the triplet manifold which results in the formation of a highly phosphorescent state.[1−5] In several nitrated aromatic compounds an additional direct reactive channel exists in parallel with the formation of T_1. This channel corresponds to a molecular rearrangement of the bonding of the NO_2 group to the aromatic rings, leading to the dissociation of nitrogen(II) oxide (NO·) and the formation of an aryoxyl radical (Ar−O·).[6−13] Since nitrated polycyclic aromatic compounds (NPAHs) are highly toxic pollutants which are eliminated from the atmosphere through photochemical processes,[14−19] and also because of the fundamental interest in the details of their highly efficient intersystem crossing, we have taken up the study of this phenomenon in 1-nitronaphthalene (1-NN) in different solvent environments through computational and experimental approaches.

The case of 1-NN is an excellent opportunity to focus on the study of the ultrafast multiplicity change in nitrated molecules. Several flash photolysis studies did not detect primary photoproducts of this compound.[2,4,20,21] Such results show that for this particular nitroaromatic, the photochemical pathway (NO· release) is practically absent and that the depopulation of S_1 is determined solely by the formation of the phosphorescent T_1 state which has been detected by $T_n \leftarrow T_1$ transient absorption,[2,4,20,21] by its phosphorescence spectrum,[1,20,22] by transient resonance Raman experiments,[21] and by the products of specific intermolecular reactions (secondary bimolecular photochemistry of the triplet including electron and hydrogen transfer).[21,23]

Recently, we realized the first experimental determinations of the emission from the first singlet excited state of several nitroaromatic compounds in methanol solution.[24] Although NPAHs are considered nonfluorescent, the molecular emission was resolved through the frequency up-conversion scheme in the subpicosecond time scale. In that study, it was observed that all nitroaromatics have very rapid fluorescence decays. As mentioned before, such behavior is dictated mainly by the intersystem crossing channel, although the NO· lose channel should add up to the depletion of the S_1 state in several of the NPAHs. In fact, it can be postulated that the rate of ISC indirectly determines the photoreactivity of NPAHs since the two channels have competing kinetics and it has been established that the dissociation products do not accumulate from the phosphorescent triplet.[9,10] Of the five nitroaromatics of our previous study, 1-NN was the only one where a single exponential was observed for the S_1 decay in methanol. In the other compounds, a structural relaxation causes the S_1 decay to slow down after the first 100 fs, since the depletion rate at the locally excited geometry is faster than at the relaxed geometry (and thus, double-exponential kinetics are observed).[24]

A preliminary steady-state spectroscopic study of 1-NN showed us that its UV−vis absorption spectrum undergoes a bathochromic shift when the solvent polarity is increased (see Results and Discussion section). Such solvent effect on the S_1

* Corresponding author. E- mail: jpeon@servidor.unam.mx.

10.1021/jp074809a CCC: $40.75
Published on Web 01/01/2008

excitation energy can, in principle, have consequences in the intersystem crossing dynamics since it is well-known that the coupling to the triplet manifold is a strong function of the relative energies between the singlet and the receiver T_n states (energy gap law).[25−29] With this in mind, we have measured the S_1 lifetimes in a series of solvents in order to observe to what extent the ultrafast decays are sensible to the polarity of the solution and to determine if the single-exponential kinetics are altered as a function of the structure of the solvent.

The excited states of 1-NN have been the subject of only one theoretical study back in 1972.[20] In that study, Mikula et al. applied the CNDO−CI methodology to calculate the singlet and triplet manifolds of 1-NN in the gas phase. The authors were able to postulate several aspects of the spectroscopy of this compound like the classification of S_1 and T_1 as ($\pi-\pi^*$) states. Additionally, the CNDO−CI calculations showed the existence of upper triplet states with contributions from the appropriate electronic configurations that promote an efficient intersystem crossing from the spectroscopic singlet (some 35 years before the present measurements with the appropriate femtosecond time resolution).

In this report we include, in addition to the measurements, a computational study about the electronically excited states of 1-NN considering the effects of several solvent environments. For this we have chosen the time-dependent density functional theory (TD−DFT)[30,31] since this is an efficient computational method which has proven to be reliable to study systems of similar size and nature as 1-NN, including two ring systems like coumarins,[32] compounds with charge-transfer states like nitrated aromatic amines,[33−36] and nucleic acid bases.[37,38] One of the most remarkable results of the recent TD−DFT methodologies is that they are able to predict the UV−vis absorption pattern of groups of small conjugated molecules (where the accuracies are particularly good when extended basis sets are used and when solvent effects are taken into account).[39−41] Additionally, the TD−DFT method has been proven to be successful in predicting photophysical effects related to the relative energies of different low-lying singlet states. For example, in references 37 and 38, this methodology was used to correlate the photophysical behavior of nucleic acid bases to the proximity of ($\pi-\pi^*$) and ($n-\pi^*$) singlets, and even to predict solvent effects in the internal conversion rates. Of particular relevance to the present study are several examples of the use of the TD−DFT theory to estimate the relative energies of the singlet and triplet manifolds of small aromatic molecules. Those studies were able to correlate the rate of intersystem crossing with the energy alignment of singlet and triplet states. Examples include the identification of singlet−triplet state crossings,[42] and several investigations about the relation between singlet−triplet energy gaps between specific pairs of states (S_1-T_n), and the singlet−triplet conversion rates.[29,43,44−47] All these studies have considered the analysis of the DFT orbitals in order to determine several properties of the electronic states which in turn define the existence of specific photophysical channels, for example, distinguishing the ($\pi-\pi^*$) character versus the ($n-\pi^*$) character of the states or identifying their charge-transfer nature.

The aim of the present computational work is to establish whether the TD−DFT formalism is able to generate a state energy diagram for the low-lying singlet and triplet states of 1-NN that is consistent with our experimental observations in regard to the solvatochromism in the absorption spectra and the ultrafast singlet depletions, as well as the solvent influence in the decay rates. We have chosen the parameter-free PBE0 hybrid functional of Adame and Barone[48] since this method, when used with a large-enough basis set, has recently shown remarkably good results in excited-state calculations and produces reliable ground-state geometries.[38,40,49,50] The solvent effects are taken into account through the Polarizable Continuum Model (PCM) where the solvent surrounding the solute cavity is modeled as a structureless medium with a specific dielectric constant and where the solvent radius and density are considered.[51−53] Our measurements were made in several solvents, ranging from nonpolar to highly polar. As representative of these, our calculations include the cases of cyclohexane, acetonitrile, and methanol as well as the gas phase.

Methodology

Experimental Methods. Methanol, pentanol, acetonitrile, and cyclohexane were high-performance liquid chromatography grade from Aldrich. 1-NN and naphthalene were purchased from Aldrich and were recrystallized from methanol before use. Absorption spectra of the solutions were acquired on a Cary-50 spectrophotometer (Varian) in 1 cm quartz cells. Time-resolved fluorescence measurements were obtained through the frequency up-conversion method. Our setup has been described in detail elsewhere.[24] Briefly, a 50 fs pulse train was generated in a Ti:sapphire oscillator. Excitation pulses were obtained by frequency doubling in a 0.5 mm BBO crystal. The polarization of the second harmonic beam was adjusted to the magic angle with a half-wave plate before it was focused into a 1 mm path length flow cell containing the samples. The average power at the cell was 4 mW (100 MHz repetition rate) at 385 nm. The fluorescence from the sample was collected and refocused with a pair of parabolic mirrors. The emission intensity was time-resolved by sum frequency mixing it with a temporally delayed 770 nm pulse in another 0.5 mm BBO crystal. The up-conversion signal was refocused into the entrance slit of a double monochromator and detected with a photomultiplier tube connected to a lock-in amplifier referenced to a 200 Hz optical chopper in the path of the pump beam. The instrument response function for our apparatus was determined to be Gaussian with a 180 fs full width at half-maximum (fwhm), through a cross-correlation measurement between the gate pulses and the Raman scattering of the pump pulses by the solvents. All experiments were performed at room temperature (20 ± 1 °C) under aerated conditions.

Computational Methods. For all the calculations, the Gaussian 03 program was used.[54] The molecular geometry of 1-NN in its electronic ground state was fully optimized at the PBE0/6-311G(d,p) level. To include the solvent effects, we used the PCM model. The default options were kept for the self-consistent field convergence and optimization thresholds. For every optimized structure we verified that all the vibrational frequencies of the system were real. For the excited-state calculations, we applied the TD−DFT method at the (PCM)-PBE0/6-311++G(d,p) level of theory directly at the ground-state optimized geometries. The use of this basis set for TD calculations seems adequate from previous studies where it was seen that the energy of the excited states has converged with this basis set.[40] Also, we verified that the use of a smaller basis set like 6-311G(d,p) yields a non-converged energy for the excitations (with an S_1 energy about 0.1 eV higher than with 6-311++G(d,p)), and that incrementing the basis set to 6-311++G(2d, 2p) changes these energies by less than 0.01 eV.

It should be noticed that, since our experimental work involves steady-state absorption spectra and sub-100 fs dynamics

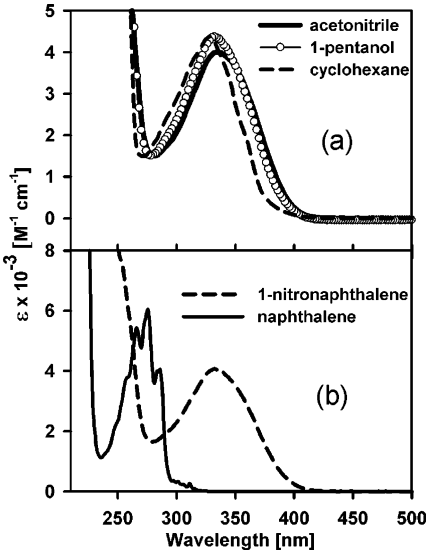

Figure 1. (a) Steady-state absorption spectra of 1-nitronaphthalene in a series of solvents. (b) Steady-state absorption spectra of 1-nitronaphthalene and naphthalene in methanol.

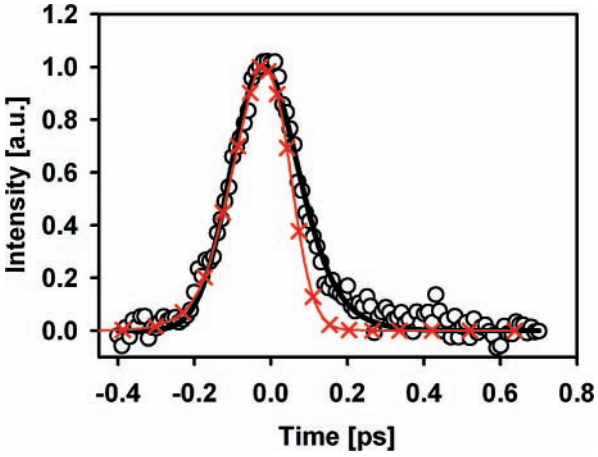

Figure 2. Circles: fluorescence up-conversion measurements of 1-nitronaphthalene in acetonitrile. The excitation wavelength was 385 nm, and the emission wavelength was 470 nm. The solid black line is a nonlinear least-squares fit to a single-exponential decay convoluted with the instrument response function. Crosses and red line: cross-correlation measurement between the gate pulse and the Raman scattering in methanol at 435 nm using the same excitation wavelength.

which occur on a time scale similar to that of molecular relaxation following a vertical excitation,[24] the chosen molecular geometries in the calculations are those of the electronic ground state (excited singlet structure immediately after vertical excitation). From a similar reasoning, we considered the nonequilibrium PCM solutions for the TD−DFT calculations. This, since some of the motions of the solvent ("solvation" other than through purely electronic redistribution and the inertial part of the solvent response), occurs on time scales longer than the photon absorption event and the ultrafast S_1 depletions that we measured. It should be noted then that the calculated energies do not correspond to the states after solvent and solute relaxation, which occur on the same or longer time scales as the S_1 depletions.

Results and Discussion

Experimental Results. The solution steady-state spectroscopy of 1-NN is markedly different from that of the parent molecule naphthalene. Figure 1a shows absorption spectra of 1-NN in a series of solvents of a wide range in polarity, while Figure 1b compares the UV−vis spectrum of 1-NN with that of naphthalene in methanol solution. Most noticeable is the fact that the first absorption band of 1-NN in all solvents has a much larger absorption coefficient than that of naphthalene's first electronic transition. The first weak absorption band in naphthalene corresponds to a nearly forbidden transition to the $^1B_{3u}$ state ($^1L_b \leftarrow {}^1A$ transition, $\lambda_{max} = 310$ nm, long-axis polarized), and the second band corresponds to a medium-intensity transition to the $^1B_{2u}$ state ($^1L_a \leftarrow {}^1A$ transition, $\lambda_{max} = 275$ nm, short-axis polarized).[55,56] On the other hand, the first absorption band in 1-NN has an absorption coefficient of about 4000 M^{-1} cm^{-1} at its maximum; also, this band appears at much longer wavelengths in comparison with naphthalene's first and second transitions. This effect, observed previously in other 1-substitued, and 1,5- or 1,8-disubstitued naphthalenes, has been described in terms of an increase in the molecular conjugation along the short molecular axis.[56] The extension of the conjugation makes the energy of the state with a transverse polarized transition moment to be reduced with respect to the electronic state with a transition moment parallel to the long molecular axis (longitudinally polarized). Examples of this trend are 1-aminonaphthalene ($\lambda_{max} = 325$ nm),[57] 1,5-dimethylnaphthalene ($\lambda_{max} = 285$ nm),[58] 1,8-dimethylnaphthalene ($\lambda_{max} = 285$ nm),[58] 1-chloronaphthalene ($\lambda_{max} = 285$ nm),[59] acenaphthene ($\lambda_{max} = 290$ nm), and perinaphthane ($\lambda_{max} = 290$ nm),[60] where in parenthesis we include the maximum of the absorption band of the respective transverse polarized transition (to be compared with the $\lambda_{max} = 275$ nm value for naphthalene).

The solution absorption spectra of 1-NN are similar to that of 1-aminonaphthalene. In both these cases it appears that the band associated with the transverse polarized transition is red-shifted by more than 55 nm and broadened in comparison with that of naphthalene. In fact, the CNDO−CI results of ref 20 as well as the TD−DFT calculations of this contribution (see computational results) predict that the first electronically excited state has a transition dipole moment which lies in the molecular plane making a small angle with respect to the inner C−C bond. Additionally, the calculated first singlet excited state has a large contribution from a HOMO−LUMO transition in 1-NN, while in naphthalene the first electronically excited singlet corresponds to the ^1L_b state.[25,56]

Looking at the spectra in Figure 1, it can be seen that there is a clear bathochromic shift when going from cyclohexane to the group of polar solvents. Due to small changes in the shapes of these spectra, the shift is particularly clear in the long-wavelength edge of the bands where it can be as large as 17 nm.

We now turn to the study of the first singlet excited-state dynamics with femtosecond resolution. In our previous report,[24] we determined the fluorescent-state lifetime of 1-NN in methanol to be of about 70 fs. Here, we extend these measurements to a series of solvents and include a measurement in methanol with improved signal-to-noise ratio. The results of our time-resolved fluorescence measurements are included in Figures 2 and 3. All these experiments correspond to an excitation wavelength of 385 nm and to the up-conversion of 470 nm fluorescence. We observed that in all the solvents, the fluorescence obeys a single-exponential decay to the baseline with the following time constants: $\tau = 60 \pm 10$ fs in methanol, $\tau = 65 \pm 10$ fs in pentanol, $\tau = 50 \pm 10$ fs in acetonitrile, and $\tau = 100 \pm 20$ fs in cyclohexane. In Figure 2, we show a comparison between the up-conversion trace in acetonitrile and the instrument function to show that the observed decays are not limited by our instrumental response.

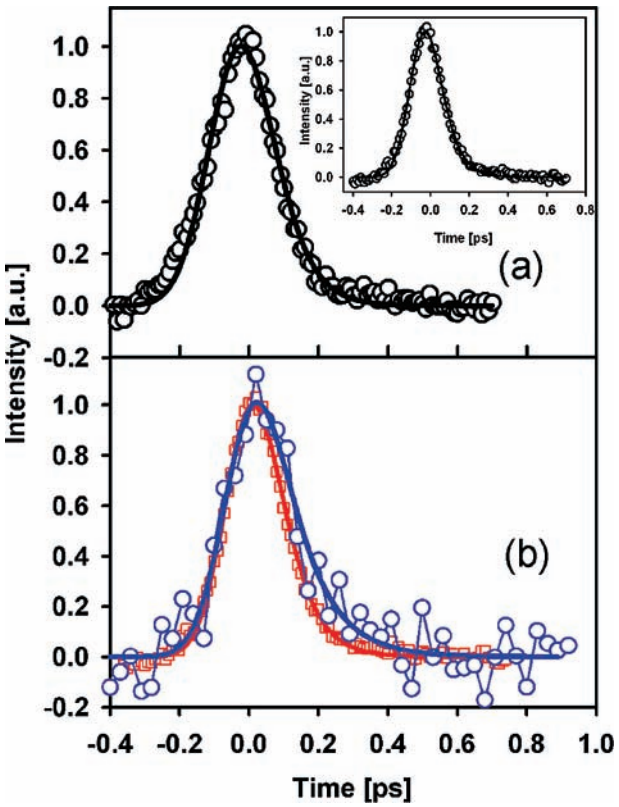

Figure 3. (a) Fluorescence up-conversion measurements of 1-nitronaphthalene in 1-pentanol (main graph) and methanol (inset). (b) Fluorescence up-conversion measurements of 1-nitronaphthalene in cyclohexane (blue) and methanol (red). In all cases, the excitation wavelength was 385 nm and the emission wavelength was 470 nm. Solid lines are nonlinear least-squares fits to a single-exponential decay convoluted with the instrument response function.

In cyclohexane, the up-conversion signal is much weaker than in the polar solvents. We attribute this to the fact that in the nonpolar solvent, the first absorption band appears shifted to the blue; therefore, it is expected that the emission band is also shifted toward shorter wavelengths, with which the fluorescence at 470 nm may correspond to the long-wavelength edge of the emission band. Attempts to isolate fluorescence signals at shorter wavelengths for 1-NN in cyclohexane failed due to the up-conversion of Raman scattering from the solvent which masked or contaminated any short-lived emission. For all the experiments of Figures 2 and 3, we carefully verified that Raman scattering does not contribute to the up-conversion near $t = 0$ through runs with the solvent-only with the same flow cell. This check was made under identical alignment conditions and in back-to-back experiments with the measurements of the respective 1-NN solutions. It should be noted that the results in methanol and pentanol are nearly identical, which demonstrates that the viscosity and size of the solvent molecules have a negligible effect and that the S_1 depletions occur before the response of the solvent shells in the alcohols (Figure 3a).

The main conclusion which can be obtained from these experiments is that the intersystem crossing channel is highly efficient in all solvents, independent of polarity and hydrogen-bonding ability. Only for the case of cyclohexane there is an increase in the excited-state lifetime in comparison with the polar solvents. In Figure 3b, we superimpose the traces in methanol and in cyclohexane to show that even with the different signal-to-noise ratios, the increase in the S_1 lifetime is clear.

The sub-100 fs fluorescence times in 1-NN appear to be an ultrafast signature of El-Sayed's rules which predict that the singlet−triplet interaction through spin−orbit coupling is highly effective when a singlet state is nearly isoenergetic with a vibro-electronic triplet state and where the change in electronic spin is accompanied by a specific change in the electronic configurations, here: $^1(\pi-\pi^*) \rightarrow {}^3(n-\pi^*)$. As will be shown next, the TD−DFT methodology permits a qualitatively correct accounting of this phenomena as it predicts the proper state ordering, the $(\pi-\pi^*)$ nature of both the first excited singlet and first triplet states, and the small energy gap between S_1 and upper receiver T_n states.

SCHEME 1: Structure and Atom Numbering of 1-Nitronaphthalene

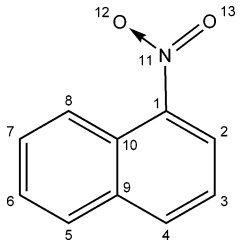

Computational Studies and Comparisons with the Experimental Results. For our computational studies, the geometry of the electronic ground state of 1-NN was optimized at the (PCM)PBE0/6-311G(d,p) level of theory. Structural data on 1-NN is not available for direct comparisons with the PBE0 geometries. However, the density functional theory has been used previously to determine the gas phase geometry of several nitroaromatic compounds,[61] and it has been observed that hybrid functionals produce good agreement with several experimentally determined parameters of other NPAHs.[62,63] The average C−N bond length of a series of NPAHs has been reported to be 1.468 Å.[63] As a comparison, in our optimized geometries the C−N distance ranges from 1.4610 Å in methanol, to 1.47083 Å in the gas phase. The calculated ground-state geometries of 1-NN actually correspond to nonplanar structures where the nitro group defines a $C_{10}-C_1-N_{11}-O_{12}$ dihedral angle of around 30° (from 31.8° in methanol, to 28.0° in the gas phase; see Scheme 1 for the atom numbering). Previous DFT calculations of nitroaromatics have indicated that this torsion is due to a steric hindrance between an oxygen atom and a peri-hydrogen in its vicinity.[61] In fact, other NPAHs, like nitrobenzene, 2-nitronaphthalene, and 2-nitroanthracene, without this nearby hydrogen atom form nearly planar structures.[61,62] In addition, as indicated previously in reference 61, in the planar nitroaromatics, the C−N and the O−N bonds are slightly shorter than in the nonplanar ones, indicating a somewhat lower NO_2 conjugation in compounds like 1-NN.

The results of our excited-state calculations are included in Table 1 and in Figure 4, where we show the energy ordering in the singlet and triplet manifolds. In the first place, the electronic excitation coefficients indicate that both the first singlet excited and first triplet states have their main contribution from transitions from the highest occupied molecular orbital HOMO (DFT orbital 45) to the lowest unoccupied molecular orbital LUMO (DFT orbital 46). This situation is maintained in the gas phase and in each of the three solvent environments. Isosurfaces of the frontier DFT orbitals of 1-NN in acetonitrile are depicted in Figure 5 (corresponding images in other environments are included as Supporting Information). The shapes of these isosurfaces do not show significant changes in either of the different solvents or in the gas phase. It can be appreciated that the HOMO orbital in all cases resembles naphthalene's a_u frontier π-orbital, and that the LUMO orbital

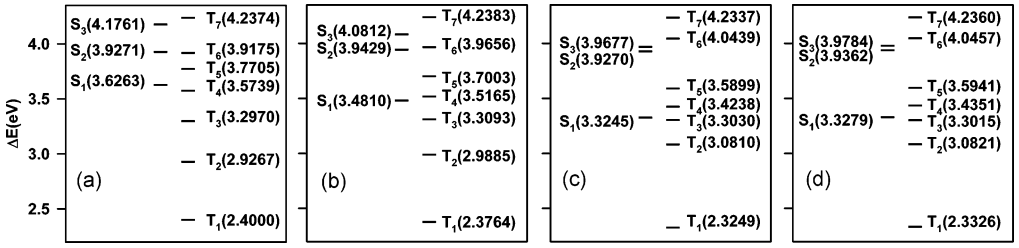

Figure 4. Excitation energy diagram of 1-nitronaphthalene at the (PCM)TD−PBE0/6-311G++(d,p) level of theory for a series of solvents and in the gas phase. The excitation energies (eV) are indicated in parentheses and were calculated at the (PCM)PBE0/6-311G(d,p) ground-state optimized geometries. (a) Gas phase, (b) cyclohexane, (c) acetonitrile, and (d) methanol.

TABLE 1: Excitation Energies (eV), Oscillator Strengths *f*, and Largest Excitation Coefficients for 1-NN in Different Environments (A−D) Computed by the (PCM)TD−PBE0/6-311++G(d,p) Method at the (PCM)PBE0/6-311G(d,p) Ground-State Geometry

singlet manifold					triplet manifold			
state	transition	coefficient	energy	*f*	state	transition	coefficient	energy
				A. Gas Phase				
1	45 → 46	0.63704	3.6263	0.1034	1	45 → 46	0.71568	2.4000
2	43 → 46	0.59934	3.9271	0.0019	2	40 → 46	0.53784	2.9267
						41 → 46	−0.51163	
3	44 → 46	0.62105	4.1761	0.0258	3	43 → 46	0.60655	3.2970
					4	44 → 46	0.64276	3.5739
					5	45 → 47	0.48376	3.7705
					6	42 → 46	0.52549	3.9175
						41 → 46	0.35235	
					7	45 → 48	0.70165	4.2374
				B. Cyclohexane				
1	45 → 46	0.65721	3.4810	0.1426	1	45 → 46	0.70672	2.3764
2	43 → 46	0.58706	3.9429	0.0001	2	40 → 46	0.75363	2.9885
3	44 → 46	0.64911	4.0812	0.0460	3	43 → 46	0.56678	3.3093
					4	44 → 46	0.64508	3.5165
					5	45 → 47	0.49840	3.7003
					6	41 → 46	0.53461	3.9656
						42 → 46	0.34871	
					7	45 → 48	0.69559	4.2383
				C. Acetonitrile				
1	45 → 46	0.66367	3.3245	0.1397	1	45 → 46	0.70326	2.3249
2	44 → 46	0.65766	3.9270	0.0411	2	40 → 46	0.76317	3.0810
3	43 → 46	0.53024	3.9677	0.0027	3	43 → 46	0.41825	3.3030
						45 → 47	0.41355	
						44 → 46	0.31351	
					4	44 → 46	0.60092	3.4238
					5	45 → 47	0.47757	3.5899
						42 → 46	0.28697	
					6	41 → 46	0.60525	4.0439
					7	45 → 48	0.50755	4.2337
				D. Methanol				
1	45 → 46	0.66345	3.3279	0.1349	1	45 → 46	0.69980	2.3326
2	44 → 46	0.65761	3.9362	0.0393	2	40 → 46	0.76885	3.0821
3	43 → 46	0.53119	3.9784	0.0025	3	45 → 47	0.43610	3.3015
						43 → 46	0.41559	
						44 → 46	0.28746	
					4	44 → 46	0.61442	3.4351
					5	45 → 47	0.45804	3.5941
						42 → 46	0.29025	
					6	41 → 46	0.60127	4.0457
					7	45 → 48	0.62815	4.2360

has a clear π^* character, localized at both the nitro group and the naphthalenic rings. The calculations show that the transition to the first singlet excited state has a significant oscillator strength of between 0.1034 in the gas phase and 0.1426 in cyclohexane, indicating an allowed transition of mid intensity.

In agreement with the experimental absorption spectra, the calculated S_1 transition energies show dependence with the solvent environment going from 3.6263 eV in the gas phase to 3.4810 eV in cyclohexane, and down to 3.3245 eV in acetonitrile. From oscillator strengths, solvent effects, and transition energies, the first singlet transition from the calculations can be readily associated with the first observed band of 1-NN in the absorption spectra of Figure 1. It should be noted that the upper calculated singlet states S_2 and S_3 appear at higher energies (below 315 nm) and have much smaller oscillator strengths. The differences between the calculated excitations for S_1 and the maxima of the first absorption band are between 0.32 eV in cyclohexane (λ_{max} = 326 nm: 3.80 eV) and 0.37 eV in methanol and acetonitrile (λ_{max} = 335 nm: 3.70 eV). Considering the HOMO−LUMO character of the S_1 state, it is clear that the nitro group makes the first electronic transition drastically change in character with respect to the case of naphthalene. That is, in 1-NN the first transition of HOMO−LUMO character is significantly red-shifted thanks to the NO_2

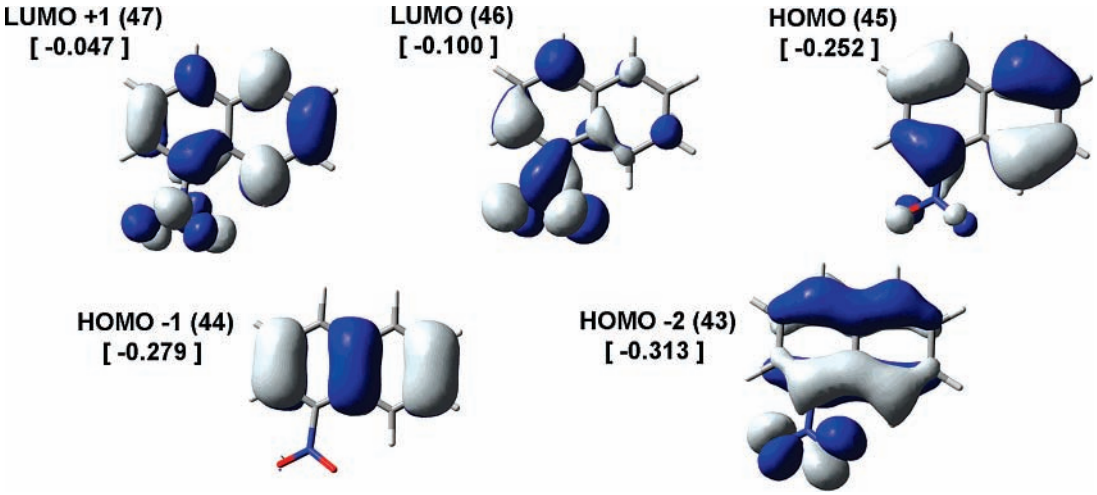

Figure 5. Isosurfaces of DFT orbitals of 1-nitronaphthalene through the PBE0 functional with the 6-311G++(d,p) basis set calculated in acetonitrile with the PCM solvation model (isosurface value: 0.03). In brackets, we include the DFT orbital energy (atomic units).

group which extends the conjugation in the short-axis direction and allows this transition to have a charge-transfer character. In the TD−PBE0 results, the transition dipole moment direction for S_1 makes a small angle of between 15.8° (in the gas phase) and 18.32° (in acetonitrile) with the short molecular axis of the ring system, showing that the first absorption band in 1-NN is nearly short-axis polarized, in agreement with the arguments of the previous section.

We now refer to the TD−PBE0 calculated states in the triplet manifold in regard to their role in the ultrafast depletion of the S_1 state. In the gas phase, the lowest four triplet states of 1-NN lie below the S_1; and in each of the three solvents, there are three triplet states below S_1. As mentioned before, the T_1 state has its main contribution from a HOMO−LUMO single-particle excitation and is classified as a $\pi-\pi^*$ state. In the three solvents and in the gas phase, the T_2 state is formed from an excitation from orbital 40 (HOMO-5), a π-orbital almost totally localized in the NO_2 group, to the LUMO orbital. The next triplet state T_3 is the state immediately below the corresponding S_1 state in the three solvents. The S_1-T_3 energy gap in the solvents ranges between 0.171 eV in cyclohexane and only 0.0215 eV in methanol. This triplet state is formed with an important contribution from an excitation from orbital HOMO-2 to the LUMO orbital.

As can be appreciated from its isosurface, the HOMO-2 orbital is formed in part from a π-orbital at the ring system (similar to the b_{3g} orbital in naphthalene), and in part from a nonbonding orbital at the oxygens (similar to the n_- (b_1) linear combination in nitromethane[64]), where this part of the orbital is aligned in the plane of the NO_2 triad with perpendicular nodal planes in the oxygen atoms. The ≈30° angle of the NO_2 plane with respect to the naphthalenic rings allows for this orbital to have contributions from both a π-type orbital and the n_- NO_2 nonbonding orbital. We have observed that when the molecule is restricted to be planar, the b_{3g}-type orbital and the n_- orbital define independent DFT orbitals, instead of mixing into the HOMO-2. Since El-Sayed's rules state that the multiplicity change becomes highly efficient when the spin−orbit interaction mixes two states which differ in both spin and electronic configuration (orbital angular momentum), the triplet state T_3 is a probable "receiver state"[20] in the intersystem crossing which determines the ultrafast S_1 depletion through a $^1(\pi-\pi^*) \rightarrow {}^3(n-\pi^*) \rightarrow {}^3(\pi-\pi^*)$ route.

Although both computational studies support the ultrafast depletion of S_1 through intersystem crossing, there are some clear qualitative and quantitative differences between the results of the CNDO−CI calculations of ref 20 and the TD−PBE0 results. First, in the calculations of Mikula et al., both the S_1 and T_1 states are $\pi-\pi^*$ and similar to naphthalene's B_{2u} state but without the charge-transfer character shown in our TD−PBE0 calculations. Also, they indicate that the most likely "receiver state" is the fourth triplet state which has about 50−50 composition of a $\sigma-\pi^*$ character and $\pi-\pi^*$character.

Since in our calculations the mixing of the n_- NO_2 orbital with the b_{3g}-type orbital into orbital 43 appears to be determined by the NO_2 orientation (lack of planarity), we made a series of TD−PBE0 calculations at other geometries to determine how sensible is the state ordering and the singlet−triplet gaps with respect to the $C_{10}-C_1-N_{11}-O_{12}$ dihedral. Specifically, we made a series of partial ground-state optimizations by restricting this dihedral to the following values: 0°, 15°, and 45°. In this part of the study, we only considered cyclohexane and acetonitrile as representative solvent environments. The results of the (PCM)TD−PBE0 calculations at the different angles (including the fully optimized case of ≈30°) are presented in Figure 6 and in the Supporting Information. In cyclohexane, in each angle, the partial ($n-\pi^*$) character of the third triplet state is maintained. That is, the largest single-particle excitation for this state is, at every angle, from orbital 43 to 46, where orbital 43 has a NO_2 nonbonding orbital character. Also, at every angle, T_3 lies below the S_1 state (at 0° and 15°, the T_4 triplet also lies below S_1, this triplet corresponds to a state with a main single-particle excitation coefficient from orbital 44 to orbital 46 and has a clear ($\pi-\pi^*$) character).

In acetonitrile, at the fixed $C_{10}-C_1-N_{11}-O_{12}$ dihedral angle of 0°, S_1 is slightly above both T_4 and T_3 (at this particular angle, the triplet with an ($n-\pi^*$) character is T_4 and T_3 is a ($\pi-\pi^*$) state). At 15°, S_1 lies just above T_3 and right below T_4, where both triplet states have some ($n-\pi^*$) character (43 to 46 single-particle excitation). At an angle of 45°, the situation is similar to the optimized geometry case (≈30°), where S_1 is above T_3, which is the state with a ($n-\pi^*$) character.

In summary, about the nitro-group alignment dependence, it can be said that while the contribution from the 43 → 46 excitation varies, a triplet state with a large ($n-\pi^*$) contribution remains a few tenths or hundreds of an eV below the S_1 state for all the NO_2 orientations. It can be concluded that this state ordering does not require a very specific orientation of the NO_2−aromatic rings. In previous studies of aromatic carbonyl compounds, it has been mentioned that a ($\pi-\pi^*$) and ($n-\pi^*$)

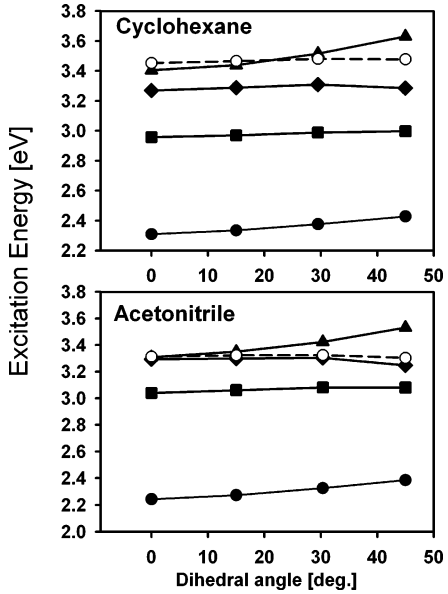

Figure 6. Excitation energies as a function of the $C_{10}-C_1-N_{11}-O_{12}$ dihedral angle in cyclohexane and in acetonitrile. Full circles, squares, diamonds, and triangles correspond, respectively, to the first to fourth triplet states, and empty circles to the lowest-energy singlet excited state.

mixing of the receiver triplet increases the degree of spin−orbit coupling,[65] so that the ultrafast singlet−triplet conversion in 1-NN might also be related to this mixing at the nonplanar geometries.

The sub-100 fs intersystem crossing in 1-NN should be placed in the context of other very rapid singlet−triplet nonradiative transitions. For example, in benzophenone, the sub-10 ps intersystem crossing time is due to the $^1(n-\pi^*) \rightarrow {}^3(\pi-\pi^*) \rightarrow {}^1(n-\pi^*)$ nature of the process.[66,67] However, for this system, several reports indicate that the receiver $^3(\pi-\pi^*)$ state is slightly above the S_1 state (10 to 50 cm^{-1}),[65,68,69] so that the rapid (picoseconds) depletion of the fluorescent state can be regarded as activated by coupling with the solvent fluctuations. In NPAHs, the S_1 decays are subpicosecond and frequently sub-100 fs, most likely due to a much larger degree of spin−orbit coupling with nearly isoenergetic upper vibronic states (probably vibrationally excited states of T_3) in the triplet manifold.

Conclusions

We have characterized the time scale of the S_1 decay of 1-NN through intersystem crossing in a series of solvents. The fluorescence times remain ultrafast in solvents of varying polarity and hydrogen-bonding ability. However, in the nonpolar solvent, the decay is about two times slower than in acetonitrile. These measurements show that 1-NN is the organic molecule with the largest intersystem crossing rate measured to date. The theoretical results at the (PCM)TD−PBE0/6-311++G(d,p) level indicate that both the first singlet excited state and the first triplet state in this molecule are of $\pi-\pi^*$ type with some aromatic-to-nitro charge-transfer character. Also, the S_1 state lies slightly above an upper triplet state with partial $(n-\pi^*)$ character. The presence of this triplet state allows the highly efficient intersystem crossing in accordance with El-Sayed's rules.

Acknowledgment. We are thankful to Professor Ahmed H. Zewail and the California Institute of Technology for the donation of equipment used in this study. For financial support we are thankful to Consejo Nacional de Ciencia y Tecnología (CONACyT, Grant 42663Q), and to Universidad Nacional Autónoma de México (UNAM, direct funding from the University Rector's Office).

Supporting Information Available: Additional computational results including fully optimized geometries, excitation energies, and transition coefficients for the partially optimized geometries, and isosurfaces of the DFT orbitals in the gas phase, methanol, and cyclohexane at the fully optimized geometries. This material is available free of charge via the Internet at http://pubs.acs.org.

References and Notes

(1) Rusakowicz, B.; Testa, A. C. *Spectrochim. Acta, Part A* **1971**, *27*, 787.
(2) Anderson, R. W.; Hochstrasser, R. M.; Lutz, H.; Scott, G. W. *Chem. Phys. Lett.* **1974**, *28*, 153.
(3) Hamanoue, K.; Hirayama, S.; Nakayama, T.; Teranishi, H. *J. Phys. Chem.* **1980**, *84*, 2074.
(4) Capellos, C.; Porter, G. *J. Chem. Soc., Faraday Trans. 2* **1974**, *70*, 1159.
(5) Hurley, R.; Testa, A. C. *J. Am. Chem. Soc.* **1968**, *90*, 1949.
(6) He, Y.; Gahlmann, A.; Feenstra, J. S.; Park, S. T.; Zewail, A. H. *Asian J. Chem.* **2006**, *1*, 56.
(7) Chapman, O. L.; Heckert, D. C.; Reasoner, J. W.; Thackaberry, S. P. *J. Am. Chem. Soc.* **1966**, *88*, 5550.
(8) Hamanoue, K.; Amano, M.; Kimoto, M.; Kajiwara, Y.; Nakayama, T.; Teranishi, H. *J. Am. Chem. Soc.* **1984**, *106*, 5993.
(9) Hamanoue, K.; Nakayama, T.; Ushida, K.; Kajiwara, K.; Yamanaka, S. *J. Chem. Soc., Faraday Trans.* **1991**, *87*, 3365.
(10) Hamanoue, K.; Nakayama, T.; Kajiwara, K.; Yamanaka, S.; Ushida, K. *J. Chem. Soc., Faraday Trans.* **1992**, *88*, 3145.
(11) Fukuhara, K.; Kurihara, M.; Miyata, N. *J. Am. Chem. Soc.* **2001**, *123*, 8662.
(12) Ioki, Y. *J. Chem. Soc., Perkin Trans. 2* **1977**, *10*, 1240.
(13) van den Braken-van Leersum, A. M.; Tintel, C.; van't Zelfde, M.; Cornelisse, J.; Lugtenburg, J. *Recl. Trav. Chim. Pays-Bas* **1987**, *106*, 120.
(14) Kim, Y.-D.; Ko, Y.-J.; Kawamoto, T.; Kim, H. *J. Occup. Health* **2005**, *47*, 261.
(15) Gerasimov, G. Y. *High Energy Chem.* **2004**, *38*, 161.
(16) Kamens, R. M.; Zhi-Hua, F.; Yao, Y.; Chen, D.; Chen, S.; Vartiainen, M. *Chemosphere* **1994**, *28*, 1623.
(17) Warner, S. D.; Farant, J.-P.; Butler, I. S. *Chemosphere* **2004**, *54*, 1207.
(18) Fan, Z.; Kamens, R. M.; Hu, J.; Zhang, J.; McDow, S. *Environ. Sci. Technol.* **1996**, *30*, 1358.
(19) Cvrčková, O.; Ciganek, M. *Polycyclic Aromat. Compd*. **2005**, *25*, 141.
(20) Mikula, J. J.; Anderson, R. W.; Harris, L. E.; Stuebing, E. W. *J. Mol. Spectrosc.* **1972**, *42*, 350.
(21) Fournier, T.; Tavender, S. M.; Parker, A. W.; Scholes, G. D.; Phillips, D. *J. Phys. Chem. A* **1997**, *101*, 5320.
(22) Wolfbeis, O. S.; Posch, W.; Gübitz, G.; Tritthart, P. *Anal. Chim. Acta* **1983**, *147*, 405.
(23) Görner, H. *J. Chem. Soc., Perkin Trans. 2* **2002**, *10*, 1778.
(24) Morales-Cueto, R.; Esquivelzeta-Rabell, M.; Saucedo-Zugazagoitia, J.; Peon, J. *J. Phys. Chem. A* **2007**, *111*, 552.
(25) Klessinger, M.; Michl, J. *Excited States and Photochemistry of Organic Molecules*; VCH: New York, 1994.
(26) El-Sayed, M. A. *J. Chem. Phys.* **1963**, *38*, 2834.
(27) Lower, S. K.; El-Sayed, M. A. *Chem. Rev.* **1966**, *66*, 199.
(28) Englman, R.; Jortner, J. *Mol. Phys.* **1970**, *18*, 145.
(29) Gigli, G.; Della Sala, F.; Lomascolo, M.; Anni, M.; Barbarella, G.; Di Carlo, A.; Lugli, P.; Cingolani, R. *Phys. Rev. Lett.* **2001**, *86*, 167.
(30) Runge, E.; Gross, E. K. U. *Phys. Rev. Lett.* **1984**, *52*, 997.
(31) Burke, K.; Werschnik, J.; Gross, E. K. U. *J. Chem. Phys.* **2005**, *123*, 062206.
(32) Cave, R. J.; Castner, E. W., Jr. *J. Phys. Chem. A* **2002**, *106*, 12117.
(33) Jamorski, C.; Foresman, J. B.; Thilgen, C.; Lüthi, H.-P. *J. Chem. Phys.* **2002**, *116*, 8761.
(34) Jamorski Jödicke, C.; Lüthi, H.-P. *J. Chem. Phys.* **2003**, *119*, 12852.
(35) Jamorski Jödicke, C.; Lüthi, H.-P. *J. Am. Chem. Soc.* **2003**, *125*, 252.
(36) Jamorski Jödicke, C.; Lüthi, H.-P. *Chem. Phys. Lett.* **2003**, *368*, 561.
(37) Mennucci, B.; Toniolo, A.; Tomasi, J. *J. Phys. Chem. A* **2001**, *105*, 4749.
(38) Gustavsson, T.; Sarkar, N.; Lazzarotto, E.; Markovitsi, D., Barone, V.; Improta, R. *J. Phys. Chem. B* **2006**, *110*, 12843.

(39) Jacquemin, D.; Preat, J.; Wathelet, V.; Fontaine, M.; Perpète, E. A. *J. Am. Chem. Soc.* **2006**, *128*, 2072.
(40) Jacquemin, D.; Perpète, E. A. *THEOCHEM* **2007**, *804*, 31.
(41) Laurent, A. D.; André, J.-M.; Perpète, E. A.; Jacquemin, D. *Chem. Phys. Lett*. **2007**, *436*, 84.
(42) Dmitrenko, O.; Reischl, W.; Bach, R. D.; Spanget-Larsen, J. *J. Phys. Chem. A* **2004**, *108*, 5662.
(43) Fabiano, E.; Della Sala, F.; Barbarella, G.; Lattante, S.; Anni, M.; Sotgiu, G.; Hättig, C.; Cingolani, R.; Gigli, G. *J. Phys. Chem. B* **2006**, *110*, 18651.
(44) Panda, D.; Mishra, P. P.; Khatua, S.; Koner, A. L.; Sunoj, R. B.; Datta, A. *J. Phys. Chem. A* **2006**, *110*, 5585.
(45) Lhiaubet, V.; Gutierrez, F.; Penaud-Berruyer, F.; Amouyal, E.; Daudey, J.-P.; Poteau, R.; Chouini-Lalanne, N.; Paillous, N. *New J. Chem.* **2000**, *24*, 403.
(46) Raganato, M. F.; Vitale, V.; Della Sala, F.; Anni, M.; Cingolani, R.; Gigli, G.; Favaretto, L.; Barbarella, G.; Weimer, M.; Görling, A. *J. Chem. Phys.* **2004**, *121*, 3784.
(47) Della Sala, F.; Heinze, H. H.; Görling, A. *Chem. Phys. Lett*. **2001**, *339*, 343−350.
(48) Adamo, C.; Barone, V. *J. Chem. Phys.* **1999**, *110*, 6158.
(49) Adamo, C.; Scuseria, G. E.; Barone, V. *J. Chem. Phys.* **1999**, *111*, 2889.
(50) Jacquemin, D.; Preat, J.; Wathelet, V.; Perpéte, E. A. *THEOCHEM* **2005**, *731*, 67.
(51) Amovilli, C.; Barone, V.; Cammi, R.; Cancès, E.; Cossi, M.; Mennucci, B.; Pomelli, C. S.; Tomasi, J. *Adv. Quantum Chem.* **1998**, *32*, 227.
(52) Cossi, M.; Barone, V. *J. Chem. Phys.* **2001**, *115*, 4708.
(53) Cossi, M.; Scalmani, G.; Rega, N.; Barone, V. *J. Chem. Phys.* **2002**, *117*, 43.
(54) Frisch, M. J.; Trucks, G. W.; Schlegel, H. B.; Scuseria, G. E.; Robb, M. A.; Cheeseman, J. R.; Montgomery, J. A., Jr.; Vreven, T.; Kudin, K. N.; Burant, J. C.; Millam, J. M.; Iyengar, S. S.; Tomasi, J.; Barone, V.; Mennucci, B.; Cossi, M.; Scalmani, G.; Rega, N.; Petersson, G. A.; Nakatsuji, H.; Hada, M.; Ehara, M.; Toyota, K.; Fukuda, R.; Hasegawa, J.; Ishida, M.; Nakajima, T.; Honda, Y.; Kitao, O.; Nakai, H.; Klene, M.; Li, X.; Knox, J. E.; Hratchian, H. P.; Cross, J. B.; Bakken, V.; Adamo, C.; Jaramillo, J.; Gomperts, R.; Stratmann, R. E.; Yazyev, O.; Austin, A. J.; Cammi, R.; Pomelli, C.; Ochterski, J. W.; Ayala, P. Y.; Morokuma, K.; Voth, G. A.; Salvador, P.; Dannenberg, J. J.; Zakrzewski, V. G.; Dapprich, S.; Daniels, A. D.; Strain, M. C.; Farkas, O.; Malick, D. K.; Rabuck, A. D.; Raghavachari, K.; Foresman, J. B.; Ortiz, J. V.; Cui, Q.; Baboul, A. G.; Clifford, S.; Cioslowski, J.; Stefanov, B. B.; Liu, G.; Liashenko, A.; Piskorz, P.; Komaromi, I.; Martin, R. L.; Fox, D. J.; Keith, T.; Al-Laham, M. A.; Peng, C. Y.; Nanayakkara, A.; Challacombe, M.; Gill, P. M. W.; Johnson, B.; Chen, W.; Wong, M. W.; Gonzalez, C.; Pople, J. A. *Gaussian 03*, revision B.03; Gaussian, Inc.: Pittsburgh, PA, 2003.
(55) Klevens, H. B.; Platt, J. R. *J. Chem. Phys.* **1949**, *17*, 470.
(56) Jaffé, H. H.; Orchin, M. *Theory and Applications of Ultraviolet Spectroscopy*; John Wiley and Sons, Inc.: New York, 1962; Chapter 13.
(57) Hirshberg, Y.; Jones, R. N. *Can. J. Res.* **1949**, *27B*, 437.
(58) Friedel, R. A.; Orchin, M. *Ultraviolet Spectra of Aromatic Compounds*; John Wiley and Sons, Inc.: New York, 1951.
(59) Ferguson, J. *J. Chem. Soc.* **1954**, 304.
(60) Platt, J. R. *J. Chem. Phys*. **1951**, *19*, 263.
(61) Onchoke, K. K.; Hadad, C. M.; Dutta, P. K. *Polycyclic Aromat. Compd*. **2004**, *24*, 37.
(62) Li, Y. S.; Fu, P. P.; Church, J. S. *J. Mol. Struct.* **2000**, *550*−*551*, 217.
(63) Allen, F. H.; Kennard, O.; Watson, D. G.; Brammer, L.; Orpen, A. G.; Taylor, R. *J. Chem. Soc., Perkin Trans. 2* **1987**, S1.
(64) Harris, D. C.; Bertolucci, M. D. *Symmetry and Spectroscopy*; Oxford University Press: New York, 1978.
(65) Ohmori, N.; Suzuki, T.; Ito, M. *J. Phys. Chem*. **1988**, *92*, 1086.
(66) Tamai, N.; Asahi, T.; Masuhara, H. *Chem. Phys. Lett*. **1992**, *198*, 413.
(67) Peon, J.; Polshakov, D.; Kohler, B. *J. Am. Chem. Soc*. **2002**, *124*, 6428.
(68) Batley, M.; Kearns, D. R. *Chem. Phys. Lett.* **1968**, *2*, 423.
(69) Morris, J. M.; Williams, D. F. *Chem. Phys. Lett.* **1974**, *25*, 312.